

# Structure, Function, and Mechanism of the Phenylacetate Pathway Hot Dog-fold Thioesterase PaaI<sup>\*S</sup>

Received for publication, December 30, 2005, and in revised form, February 6, 2006. Published, JBC Papers in Press, February 7, 2006, DOI 10.1074/jbc.M513896200

Feng Song<sup>‡</sup>, Zhihao Zhuang<sup>†1</sup>, Lorenzo Finci<sup>‡</sup>, Debra Dunaway-Mariano<sup>‡2</sup>, Ryan Kniewel<sup>§</sup>, John A. Buglino<sup>§</sup>, Veronica Solorzano<sup>§</sup>, Jin Wu<sup>¶</sup>, and Christopher D. Lima<sup>§</sup>

From the <sup>‡</sup>Department of Chemistry, University of New Mexico, Albuquerque, New Mexico 87131, <sup>§</sup>Structural Biology Program, Sloan-Kettering Institute, New York, New York 10021, and <sup>¶</sup>Department of Biochemistry, Weill Medical College of Cornell University, New York, New York 10021

The structure and biochemical function of the hot dog-fold thioesterase PaaI operative in the aerobic phenylacetate degradation pathway are examined. PaaI showed modest activity with phenylacetyl-coenzyme A, suggestive of a role in coenzyme A release from this pathway intermediate in the event of limiting downstream pathway enzymes. Minimal activity was observed with aliphatic acyl-coenzyme A thioesters, which ruled out PaaI function in the lower phenylacetate pathway. PaaI was most active with ring-hydroxylated phenylacetyl-coenzyme A thioesters. The x-ray crystal structure of the *Escherichia coli* thioesterase is reported and analyzed to define the structural basis of substrate recognition and catalysis. The contributions of catalytic and substrate binding residues, thus, identified were examined through steady-state kinetic analysis of site-directed mutant proteins.

Aromatic compounds serve as a rich source of carbon and energy for a wide variety of microorganisms and plants (1). The enzymes that make up the aromatic catabolic pathways are useful for bioremediation of environmental aromatic pollutants (1–11) and for chemical synthesis (3, 12–15). Studies of the aromatic pathways operative in common bacteria such as *Escherichia coli* and *Pseudomonas putida* (16, 17) have provided a framework against which novel pathways of environmental bacteria can be understood (18, 19). In this paper, we focus on a pathway for aerobic phenylacetate degradation. Phenylacetate derives primarily from phenylalanine, but it is also formed in degradation pathways that target a variety of environmental aromatics of natural and synthetic origin and, thus, is the central element of an important catabolon (20–22).

The gene clusters that encode the phenylacetate pathway enzymes typically contain structural genes, regulatory genes, and transport genes (17, 19, 20, 22–27). In *E. coli*, the 14 open reading frame cluster includes the structural genes *paaABCDEFGHIJKXYZ* (23). Only one of these genes, *paaK*, has been assigned function through isolation and kinetic characterization of its protein product, phenylacetate-CoA ligase (20,

23, 28, 29). This ligase catalyzes the first committed step of the pathway, which is the conversion of the ring acetate group to the corresponding CoA thioester (28, 29) (Fig. 1). Phenylacetyl-CoA then induces the synthesis of the other pathway enzymes (30, 31). The reactions catalyzed by these enzymes have been investigated but not firmly demonstrated (32). Nevertheless, a working model that incorporates the findings from the studies of both the phenylacetate pathway (32) and the analogous benzoate pathway of *Azoarcus evansii* (26, 33, 34) can be inferred (Fig. 1). According to this model, the PaaABCD enzyme complex catalyzes the addition of oxygen across the ring C(1)=C(2) bond of phenylacetyl-CoA followed by reduction to the dihydrodiol (32). The next hypothetical step is ring opening to the C-8 aldehyde, which is converted to the corresponding acid. The ensuing CoA thiolitic cleavage forms a C-6 CoA ester (32), which is processed via  $\beta$ -oxidation by enzymes of the crotonase superfamily (35, 36).

The one gene of the pathway gene cluster, *paaABCDEFGHIJKXYZ*, that does not have a defined role in phenylacetate degradation is *paaI*. The protein product PaaI is a member of the hot dog-fold enzyme superfamily (37, 38). Moreover, it belongs to the acyl-CoA thioesterase subfamily and, in particular, to the same clade of acyl-CoA thioesterases as does the *Arthrobacter* 4-hydroxybenzoyl-coenzyme A thioesterase (4-HBA-CoA thioesterase)<sup>3</sup> (39, 40). Acyl-CoA thioesterases generally function in the cell to release the carboxylate unit for degradation, export (39, 41–45), or regulation (43, 46–48) and/or to release the CoA in thioester metabolites for participation in alternate metabolic pathways (26).

In this paper we report and interpret the results from substrate screens of *A. evansii* and *E. coli* PaaI to define the biochemical role of PaaI in the context of the phenylacetate pathway. The x-ray structure of the *E. coli* apo PaaI is also reported. The *E. coli* PaaI and *Thermus thermophilus* PaaI (49) structures are analyzed in the context of the PaaI substrate specificity profile and the kinetic properties of the PaaI active site mutants. A mechanism for PaaI substrate recognition and catalysis is proposed.

## MATERIALS AND METHODS

**Chemicals**—All restriction enzymes and the T4 DNA ligase were purchased from Invitrogen. *Pfu Turbo* DNA polymerase was purchased from Stratagene. Oligonucleotide primers were custom-synthesized by Invitrogen. DNA sequencing was performed by the DNA Sequencing Facility of the University of New Mexico. Acetyl-CoA, crotonyl-CoA, methylmalonyl-CoA, *n*-butyryl-CoA, isobutyryl-CoA,  $\beta$ -hydroxybutyryl-CoA, *n*-hexanoyl-CoA, and phenylacetyl-CoA were purchased

\* This work was supported in part by National Institutes of Health Grants GM28688 (to D. D.-M.) and 1P50 GM62529 (to C. D. L.) and by the Arnold and Mabel Beckman Foundation and Rita Allen Foundation (to C. D. L.). The costs of publication of this article were defrayed in part by the payment of page charges. This article must therefore be hereby marked "advertisement" in accordance with 18 U.S.C. Section 1734 solely to indicate this fact.

<sup>S</sup> The on-line version of this article (available at <http://www.jbc.org>) contains supplemental material.

The atomic coordinates and structure factors (code 2FS2) have been deposited in the Protein Data Bank, Research Collaboratory for Structural Bioinformatics, Rutgers University, New Brunswick, NJ (<http://www.rcsb.org/>).

<sup>1</sup> Present address: Dept. of Chemistry, 415 Wartik Laboratory, Pennsylvania State University, University Park, PA 16802.

<sup>2</sup> To whom correspondence should be addressed. Tel.: 505-277-3383; Fax: 505-277-6202; E-mail: dd39@unm.edu.

<sup>3</sup> The abbreviations used are: 4-HBA, 4-hydroxybenzoate; CoA, coenzyme A; DTT, dithiothreitol; ESI, electrospray ionization; HPLC, high performance liquid chromatography; PDB, Protein Data Bank; WT, wild type.



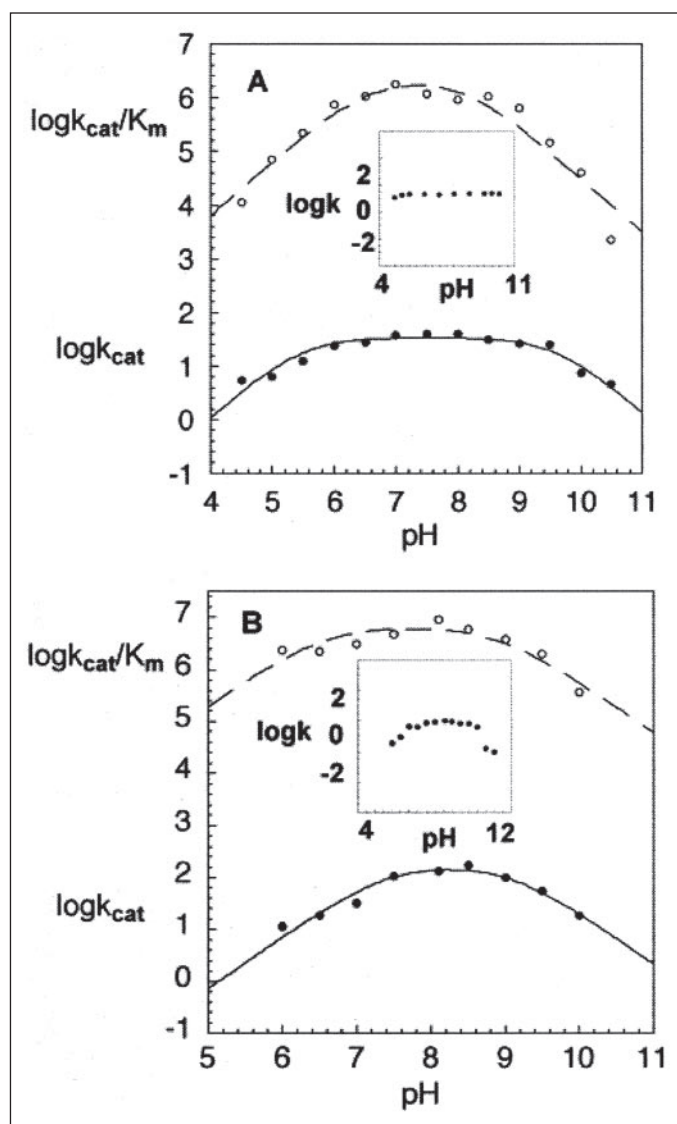


FIGURE 2. A, pH rate profiles of *A. evansii* PaaI-catalyzed hydrolysis of 3,4-dihydroxyphenylacetyl-CoA, with the inset showing a plot of the *A. evansii* PaaI activity assayed at pH 7.5 after 2 min of incubation in buffers used in the pH rate profile determinations. B, pH rate profiles of *E. coli* PaaI-catalyzed hydrolysis of 3,4-dihydroxyphenylacetyl-CoA with the inset showing a plot of the *E. coli* PaaI activity assayed at pH 8.1 after 2 min of incubation in buffers used in the pH rate profile determinations. ○,  $\log k_{cat}/K_m$ ; ●,  $\log k_{cat}$ .

*E. coli* PaaI. A solution of 10 mM  $K^+$ Hepes (pH 7.5) containing 0.15 M KCl and 1 mM DTT was used to elute the column at a flow rate of 1 ml/min. The retention time of the *E. coli* PaaI was 52.3 min versus 47.0 min for the *A. evansii* PaaI. The activities of the *A. evansii* PaaI mutants were measured before and after chromatography and found to be identical, thereby demonstrating that the protein purification protocol described above removes *E. coli* PaaI from the *A. evansii* PaaI.

**Molecular Size Determination**—The molecular mass was calculated from the amino acid composition, derived from the gene sequence, by using the EXPASY Molecular Biology Server program Compute pI/Mw. The molecular mass was measured by ESI mass spectrometry and by SDS-PAGE (4% stacking gel and 18% separating gel). The mass of native PaaI was estimated by fast protein liquid chromatography gel filtration column chromatography carried out as described in the previous section. Commercial protein molecular weight standards (Amersham Biosciences) were used to generate a plot of  $\log M_r$  versus elution volume from the column.

**Kinetic Assays**—Steady-state kinetic methods were used to determine the  $k_{cat}$  and  $K_m$  for wild-type and mutant PaaI as a function of substrate screening, reaction solution pH, or presence of an inhibitor. The details of each experimental measurement are provided in the supplemental material. The *A. evansii* PaaI reactions were typically monitored at 25 °C by using a 5,5'-dithio-bis(2-nitrobenzoic acid)-based assay in which the absorbance of 5-thio-2-nitrobenzoate at 412 nm ( $\Delta\epsilon = 13.6 \text{ mM}^{-1}\cdot\text{cm}^{-1}$ ) was measured. For *E. coli* PaaI, which is rapidly inactivated by 5,5'-dithio-bis(2-nitrobenzoic acid) under assay conditions, a continuous spectrophotometric assay was employed. Accordingly, the decrease in solution absorbance at 236 nm was monitored for the reaction mixtures of 4-hydroxyphenylacetyl-CoA ( $\Delta\epsilon = 4.2 \text{ mM}^{-1}\cdot\text{cm}^{-1}$ ), 3-hydroxyphenylacetyl-CoA ( $\Delta\epsilon = 3.6 \text{ mM}^{-1}\cdot\text{cm}^{-1}$ ), and 3,4-dihydroxyphenylacetyl-CoA ( $\Delta\epsilon = 3.2 \text{ mM}^{-1}\cdot\text{cm}^{-1}$ ). For the phenylacetyl-CoA substrates, a fixed-time, reversed-phase HPLC-based assay was used.

The initial velocity data, measured as a function of substrate concentration, were analyzed using Equation 1,

$$V = V_{\max} [S]/([S] + K_m) \quad (\text{Eq. 1})$$

where  $V$  is initial velocity,  $V_{\max}$  is maximum velocity,  $[S]$  is substrate concentration, and  $K_m$  is the Michaelis constant. The  $k_{cat}$  was calculated from  $V_{\max}/[E]$ , where  $[E]$  is the total enzyme concentration (determined using the Bradford method (62)). The inhibition constant  $K_i$  was obtained by fitting the initial rates to Equation 2,

$$V = V_{\max} [S]/[K_m (1 + [I]/K_i) + [S]] \quad (\text{Eq. 2})$$

where  $[I]$  is the concentration of the inhibitor, and  $K_i$  is the inhibition constant. The  $\log k_{cat}$  and  $\log(k_{cat}/K_m)$  values obtained from the pH rate profile analysis were fitted using Equation 3,

$$\log Y = \log(C/(1 + [H]/K_a + K_b/[H])) \quad (\text{Eq. 3})$$

where  $Y$  is  $k_{cat}$  or  $k_{cat}/K_m$ ,  $[H]$  is the hydrogen ion concentration,  $C$  is the pH independent value of  $k_{cat}$  or  $k_{cat}/K_m$ ,  $K_a$  is the acid dissociation constant, and  $K_b$  is the base dissociation constant. Data analysis was carried out using the computer program KinetAsyst (IntelliKinetics). The reported error was computed for the data fitting.

## RESULTS AND DISCUSSION

**Recombinant *A. evansii* and *E. coli* PaaI Characterization**—The theoretical molecular weights of the *A. evansii* (154 amino acids) and *E. coli* (140 amino acids) PaaIs are 16,550 and 14,851, respectively, which compare with the ESI mass spectrometric determined molecular weights of 16,419 and 14,720. Both recombinant proteins have, thus, lost the N-terminal Met (−131 Da) by post-translational modification. The *A. evansii* and *E. coli* PaaIs migrate on SDS-PAGE gels as 15- and 14-kDa proteins, whereas the native molecular masses determined by gel filtration chromatography correspond to 67 and 58 kDa. Both PaaIs are, therefore, homotetramers.

The pH rate profiles of PaaI-catalyzed 3,4-dihydroxyphenylacetyl-CoA hydrolysis (identified as the most active substrate; see below) were measured using initial-velocity techniques (Fig. 2). Both PaaIs are stable at pH 6–10 (Fig. 2, insets) and most active at pH 6–9. The bell-shaped curves were fitted to define the apparent  $pK_a$  values for ionization of essential residues in the enzyme-substrate complex ( $\log(k_{cat})$ ) and in the uncomplexed enzyme and substrate ( $\log(k_{cat}/K_m)$ ). The *A. evansii* PaaI  $\log(k_{cat})$  profile defines a  $pK_a$  of  $5.5 \pm 0.2$  ( $7.4 \pm 0.2$  for *E. coli* PaaI) for ionization of an essential base and an apparent  $pK_a$  of  $9.6 \pm 0.2$  ( $9.1 \pm 0.2$  for *E. coli* PaaI) for ionization of an essential acid. The *A. evansii* PaaI

TABLE 1

Steady-state kinetic constants for *A. Evansii* DSM6898 Paal wild-type and its mutant-catalyzed hydrolysis of acyl-CoA thioesters at 25 °C, pH 7.5

The reported error limits were computed for the S.E. in the data fitting. The reproducibility of the measured value in repeated trials is within 10% error, whereas in independent experiments the values may vary on average of 50%.

Enzyme	Substrate	$k_{cat}$ $s^{-1}$	$K_m$ $\mu M$	$k_{cat}/K_m$ $M^{-1}\cdot s^{-1}$	$K_i$ $\mu M$
WT	3,4-Dihydroxyphenylacetyl-CoA	$(1.8 \pm 0.1) \times 10^1$	$(5.1 \pm 0.2) \times 10^1$	$4 \times 10^5$	
WT	3,5-Dihydroxyphenylacetyl-CoA	$2.3 \pm 0.1$	$(2.8 \pm 0.4) \times 10^1$	$8 \times 10^4$	
WT	4-Hydroxyphenylacetyl-CoA	$(1.1 \pm 0.1) \times 10^1$	$(5.5 \pm 0.6) \times 10^1$	$2 \times 10^5$	
WT	3-Hydroxyphenylacetyl-CoA	$8.2 \pm 0.4$	$(8 \pm 1) \times 10^1$	$1 \times 10^5$	
WT	Phenylacetyl-CoA	$3.7 \pm 0.2$	$(3.9 \pm 0.5) \times 10^2$	$1 \times 10^4$	
WT	4-Hydroxybenzoyl-CoA	No activity			$(2.6 \pm 0.5) \times 10^2$
WT	3-Hydroxybenzoyl-CoA	No activity			
WT	4-Hydroxybenzyl-CoA	No activity			$3.4 \times 10^3$
WT	4-Hydroxyphenacyl-CoA	No activity			$(3.9 \pm 0.3) \times 10$
WT	3-Hydroxyphenacyl-CoA	No activity			$(2.9 \pm 0.6) \times 10$
WT	4-Chlorobenzoyl-CoA	No activity			
WT	4-Methoxybenzoyl-CoA	No activity			
WT	Acetyl-CoA	$(6.2 \pm 0.1) \times 10^{-2}$	$(1.7 \pm 0.1) \times 10^3$	$4 \times 10^1$	
WT	<i>n</i> -Hexanoyl-CoA	$(3.2 \pm 0.1) \times 10^{-2}$	$(1.6 \pm 0.2) \times 10^3$	$2 \times 10^1$	
WT	<i>n</i> -Butyryl-CoA	$(8.7 \pm 0.2) \times 10^{-2}$	$(1.2 \pm 0.1) \times 10^3$	$7 \times 10^1$	
WT	Isobutyryl-CoA	$(2.8 \pm 0.1) \times 10^{-1}$	$(1.5 \pm 0.1) \times 10^3$	$2 \times 10^2$	
WT	$\beta$ -Hydroxybutyryl-CoA	$(1.7 \pm 0.1) \times 10^{-2}$	$(6.8 \pm 0.4) \times 10^2$	$3 \times 10^1$	
WT	Methylmalonyl-CoA	$(4.7 \pm 0.2) \times 10^{-2}$	$(1.1 \pm 0.1) \times 10^3$	$4 \times 10^1$	
WT	Crotonyl-CoA	$(4.9 \pm 0.2) \times 10^{-3}$	$(1.8 \pm 0.2) \times 10^3$	3	
D75A	3,4-Dihydroxyphenylacetyl-CoA	$<1.0 \times 10^{-3}$			
D75N	3,4-Dihydroxyphenylacetyl-CoA	$(6.5 \pm 0.2) \times 10^{-3}$	$(4.8 \pm 0.3) \times 10$	$1 \times 10^2$	
N60A	3,4-Dihydroxyphenylacetyl-CoA	$(1.2 \pm 0.1) \times 10^{-2}$	$8.6 \pm 0.9$	$1 \times 10^3$	
N60D	3,4-dihydroxyphenylacetyl-CoA	$(1.8 \pm 0.1) \times 10^{-1}$	$(5.5 \pm 0.6) \times 10$	$3 \times 10^3$	

TABLE 2

Steady-state kinetic constants for *E. coli* Paal wild-type and mutant-catalyzed hydrolysis of phenylacetyl-CoA and hydroxyphenylacetyl-CoA derivatives at 25 °C, pH 8.1

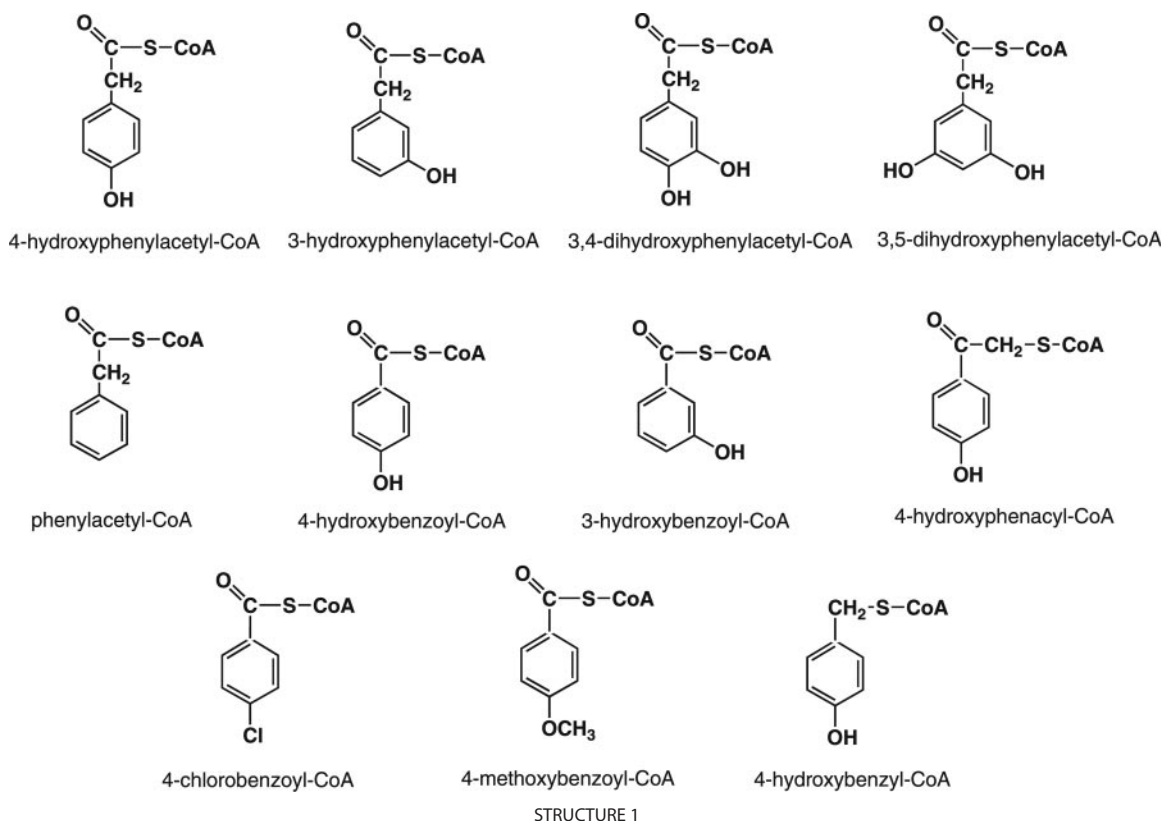
The reported error limits were computed for the S.E. in the data fitting. The reproducibility of the measured value in repeated trials is within 10% error, whereas in independent experiments the values may vary on average of 50%.

Enzyme	Substrate	$k_{cat}$ $s^{-1}$	$K_m$ $\mu M$	$k_{cat}/K_m$ $M^{-1}\cdot s^{-1}$
WT	3,4-Dihydroxyphenylacetyl-CoA	$(1.0 \pm 0.1) \times 10^2$	$(1.6 \pm 0.3) \times 10$	$7 \times 10^6$
WT	4-Hydroxyphenylacetyl-CoA	$(7.9 \pm 0.3) \times 10$	$(3.5 \pm 0.3) \times 10$	$2 \times 10^6$
WT	3-Hydroxyphenylacetyl-CoA	$(8.6 \pm 0.2) \times 10$	$(2.1 \pm 0.2) \times 10$	$4 \times 10^6$
WT	3,5-Dihydroxyphenylacetyl-CoA	$9 \pm 1$	$(2.0 \pm 0.6) \times 10^2$	$5 \times 10^4$
WT	Phenylacetyl-CoA	$(4.1 \pm 0.1) \times 10^{-1}$	$9.6 \pm 0.9$	$4 \times 10^4$
WT	4-Hydroxybenzoyl-CoA	No activity		
WT	4-Hydroxybenzyl-CoA	No activity		
WT	4-Hydroxyphenacyl-CoA	No activity		
D61A	3,4-Dihydroxyphenylacetyl-CoA	$4.4 \times 10^{-3}$		
N46A	3,4-Dihydroxyphenylacetyl-CoA	$(7.6 \pm 0.2) \times 10^{-2}$	$(2.4 \pm 0.3) \times 10$	$3 \times 10^3$
N46A	4-Hydroxyphenylacetyl-CoA	$(3.1 \pm 0.3) \times 10^{-1}$	$(2.8 \pm 0.5) \times 10^2$	$1 \times 10^3$
N46A	3-Hydroxyphenylacetyl-CoA	$(8.1 \pm 0.5) \times 10^{-1}$	$(2.3 \pm 0.3) \times 10^2$	$4 \times 10^3$
E14A	3,4-Dihydroxyphenylacetyl-CoA	$(2.0 \pm 0.1) \times 10$	$(1.3 \pm 0.2) \times 10^2$	$2 \times 10^5$
E14A	4-Hydroxyphenylacetyl-CoA	$(1.9 \pm 0.1) \times 10$	$(9 \pm 2) \times 10$	$2 \times 10^5$
E14A	3-Hydroxyphenylacetyl-CoA	$(1.5 \pm 0.1) \times 10$	$(8 \pm 1) \times 10$	$2 \times 10^5$
N15A	3,4-Dihydroxyphenylacetyl-CoA	$(2.6 \pm 0.1) \times 10$	$(4.7 \pm 0.3) \times 10$	$6 \times 10^5$
N15A	4-Hydroxyphenylacetyl-CoA	$3.2 \pm 0.1$	$(1.8 \pm 0.1) \times 10$	$2 \times 10^5$
N15A	3-Hydroxyphenylacetyl-CoA	$(3.0 \pm 0.1) \times 10$	$(3.4 \pm 0.4) \times 10$	$9 \times 10^5$
D16A	3,4-Dihydroxyphenylacetyl-CoA	$(1.1 \pm 0.1) \times 10^{-1}$	$(3.3 \pm 0.6) \times 10$	$3 \times 10^3$
D16A	4-Hydroxyphenylacetyl-CoA	$(1.7 \pm 0.1) \times 10^{-1}$	$(2.5 \pm 0.2) \times 10^2$	$7 \times 10^2$
D16A	3-Hydroxyphenylacetyl-CoA	$(6.5 \pm 0.2) \times 10^{-2}$	$(9.0 \pm 0.8) \times 10$	$7 \times 10^2$
H52A	3,4-Dihydroxyphenylacetyl-CoA	$2.7 \pm 0.1$	$(4.5 \pm 0.2) \times 10$	$6 \times 10^4$
H52A	4-Hydroxyphenylacetyl-CoA	$(2.6 \pm 0.2) \times 10^{-1}$	$(2.8 \pm 0.5) \times 10$	$9 \times 10^3$
H52A	3-Hydroxyphenylacetyl-CoA	$(8.9 \pm 0.5) \times 10^{-1}$	$(3.2 \pm 0.4) \times 10$	$3 \times 10^4$

$\log(k_{cat}/K_m)$  defines an apparent  $pK_a$  of  $6.5 \pm 0.3$  ( $6.5 \pm 0.3$  for *E. coli* Paal) for ionization of an essential base and an apparent  $pK_a$  of  $8.2 \pm 0.2$  ( $9.0 \pm 0.23$  for *E. coli* Paal) for ionization of an essential acid. The substrate ring hydroxyl group ionizes with a  $pK_a = 9.8$ , as determined by pH titration monitored at 300 nm (data not shown) and, therefore, does not contribute to the  $\log(k_{cat}/K_m)$  pH profiles. The pH profiles define the optimum pH for catalytic function, and in well defined systems they can be used to identify substrate binding or catalytic residues. Under the section "Catalytic Site of the *E. coli* Paal" (below) the active site residues that might contribute to the observed pH profiles are identified.

*Paal Substrate Screen for Determination of Biochemical Function*—The object of this substrate screen was to identify acyl-CoA thioesters that have  $k_{cat}/K_m$  values in a range that would be considered to be "physiologically relevant." The  $k_{cat}/K_m$  values of metabolic enzymes that have reached catalytic perfection are as large as  $1 \times 10^8 M^{-1}\cdot s^{-1}$ , but for most enzymes the value is  $\sim 1 \times 10^6 M^{-1}\cdot s^{-1}$ , and for those enzymes that function in secondary metabolic pathways, the value can be as low as  $1 \times 10^4 M^{-1}\cdot s^{-1}$  (63). The steady-state kinetic constants measured for the aryl-CoA and aliphatic acyl-CoA thioesters tested as substrates for *A. Evansii* and *E. coli* Paals are summarized in Tables 1 and 2, respec-

## Phenylacetate Pathway Thioesterase



tively. The aliphatic acyl-CoA thioesters screened with the *A. Evansii* PaaI are acetyl-CoA, *n*-hexanoyl-CoA, *n*-butyryl-CoA, isobutyryl-CoA,  $\beta$ -hydroxybutyryl-CoA, crotonyl-CoA, and methylmalonyl-CoA. Although these compounds were hydrolyzed, the small  $k_{\text{cat}}$  ( $1 \times 10^{-1}$  to  $1 \times 10^{-3} \text{ s}^{-1}$ ) and large  $K_m$  ( $\sim 1 \text{ mM}$ ) values show that they are not the intended substrates ( $k_{\text{cat}}/K_m$  values are  $\sim 1 \times 10^2 \text{ M}^{-1}\cdot\text{s}^{-1}$ ).

The aryl-CoA thioesters 4-chlorobenzoyl-CoA, 4-methoxybenzoyl-CoA, 4-hydroxybenzoyl-CoA, and 3-hydroxybenzoyl-CoA (structures shown in Structure 1) were tested to determine whether PaaI hydrolyzes aromatic thioesters in which the thioester group is directly attached to the aromatic ring. Such is the case with the *Arthrobacter* sp. strain SU 4-HBA-CoA thioesterase, which is the closest homolog to PaaI, having known catalytic function (39). None of these substituted benzoyl-CoA thioesters were, however, hydrolyzed by PaaI. Together, the results suggested that the PaaI does not target aliphatic acyl-CoA thioesters nor are they functionally related to the benzoyl-CoA thioesterases that participate in benzoate-based metabolic pathways (26, 39, 64) including the genisate pathway (42).

The next set of substrates screened contained the phenylacetyl-CoA structural core (Structure 1). Phenylacetyl-CoA is a fair substrate ( $k_{\text{cat}}/K_m = 1 \times 10^4 \text{ M}^{-1}\cdot\text{s}^{-1}$  for *A. Evansii* PaaI and  $4 \times 10^4 \text{ M}^{-1}\cdot\text{s}^{-1}$  for *E. coli* PaaI) (Tables 1 and 2). This result shows that the phenyl ring and its spacing from the thioester group are important determinants of PaaI substrate recognition. 2-Hydroxyphenylacetate had been reported to accumulate as a dead-end product in a mutant lacking the ring-cleaving enzyme (32) (see Fig. 1). The precursor, 2-hydroxyphenylacetyl-CoA, might therefore be targeted by PaaI. Despite the numerous strategies tried (including the procedure reported in Alonso *et al.* (65)), we were not successful at the chemical synthesis of 2-hydroxyphenylacetyl-CoA. We were, however, able to generate the target compound transiently using *E. coli* phenylacetate-CoA ligase (which was isolated for this pur-

pose) to catalyze the reaction between 2-hydroxyphenylacetate, MgATP, and CoA (in 50 mM  $\text{K}^+$ Hepes buffer (pH 7.5), 25 °C). The reaction was monitored by HPLC to show that the 2-hydroxyphenylacetyl-CoA was formed but that it was quickly hydrolyzed to 2-hydroxyphenylacetate and CoA. The chemical instability of 2-hydroxyphenylacetyl-CoA might be attributed to nucleophilic catalysis by the *ortho* ring-hydroxyl group, which is positioned to attack the carbonyl carbon of the acetyl-CoA unit, forming a lactone that undergoes subsequent hydrolysis. Insofar as the reaction conditions used here might mimic those in the cell, it would appear that the spontaneous hydrolysis of the 2-hydroxyphenylacetyl-CoA obviates the need for a dedicated thioesterase. On the other hand, we cannot rule out the possibility that the time frame of cellular chemistry might demand such a catalyst.

Although we were unable to evaluate the substrate activity of the 2-hydroxyphenylacetyl-CoA, the mono- and dihydroxylated compounds 4-hydroxyphenylacetyl-CoA, 3-hydroxyphenylacetyl-CoA, 3,4-dihydroxyphenylacetyl-CoA, and 3,5-dihydroxyphenylacetyl-CoA were found to be excellent substrates for both PaaIs (Tables 1 and 2), with  $k_{\text{cat}}/K_m \sim 1 \times 10^5 \text{ M}^{-1}\cdot\text{s}^{-1}$  for *A. Evansii* PaaI and  $\sim 1 \times 10^6 \text{ M}^{-1}\cdot\text{s}^{-1}$  for *E. coli* PaaI. The C(3) and/or C(4)-ring hydroxylation increases the reactivity by 2 orders of magnitude. For the *E. coli* PaaI, this is primarily a  $k_{\text{cat}}$  effect, whereas in the case of the *A. Evansii* PaaI, the  $k_{\text{cat}}$  and  $K_m$  are equally impacted. The PaaIs, although not identical in catalytic efficiency, appear to be tailored for catalysis of hydroxyphenylacetyl-CoA hydrolysis.

The results from the present substrate screen provide insights into PaaI biochemical function. First, given that PaaI is only minimally active toward aliphatic acyl-CoA substrates, it is unlikely that it participates in the phenylacetate lower pathway (Fig. 1). Second, the rate of catalyzed hydrolysis of phenylacetyl-CoA is adequate for CoA release in the event that the pathway ring dioxygenase-reductase becomes limiting (Figs. 1 and 3). An analogous function has been suggested for the hot dog-fold

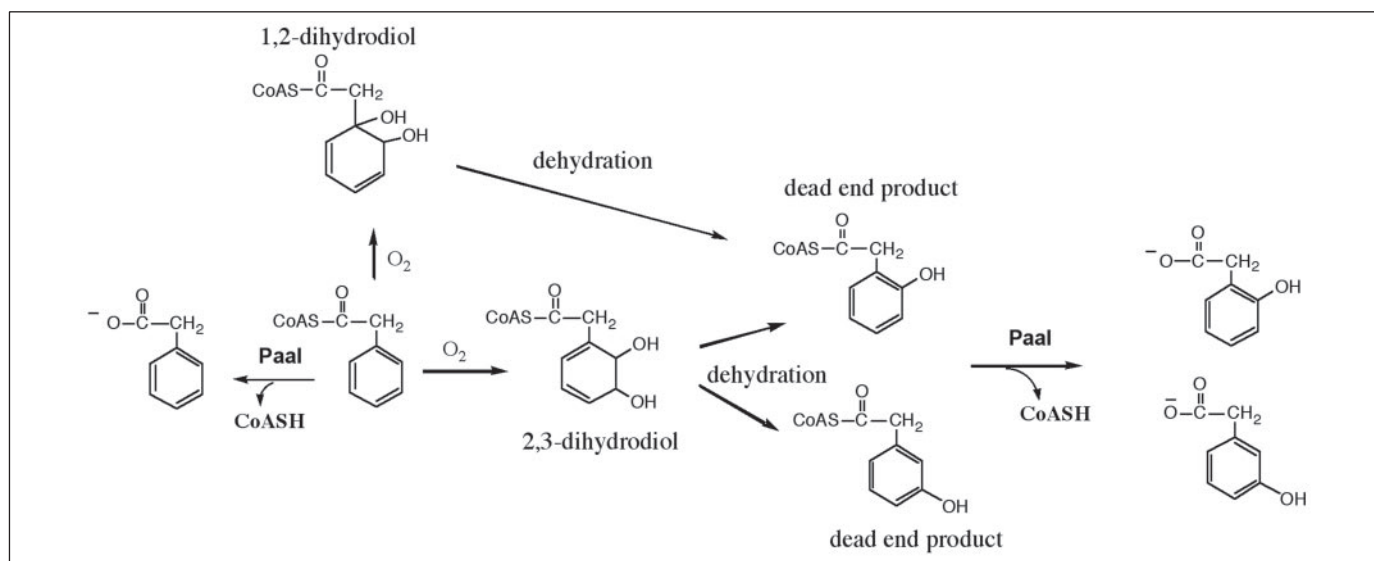


FIGURE 3. A diagram showing possible Paal substrates derived from hypothetical chemical transformations originating from the phenylacetate pathway.

thioesterase of the benzoate metabolic pathway (26). Third, the high catalytic efficiency exhibited toward ring-hydroxylated phenylacetyl-CoA indicates that Paal is poised to liberate CoA from dead-end products. Specifically, if the phenylacetate pathway proceeds via the novel 1,2-dihydrodiol intermediate as proposed (26, 32) and if catalysis by the ring opening enzyme must compete with spontaneous dehydration to the dead-end product 2-hydroxyphenylacetyl-CoA as suggested in Mohamed (29), then the Paal thioesterase might serve in a salvage capacity to release CoA and 2-hydroxyphenylacetate for alternate reaction pathways (Fig. 3). Similarly, if the phenylacetate pathway proceeds via a 2,3-dihydrodiol rather than the putative 1,2-dihydrodiol (this pathway alternative has not been ruled out) and if the 2,3-dihydrodiol undergoes spontaneous dehydration before undergoing ring cleavage, the Paal might function to release CoA from 2- and 3-hydroxyphenylacetyl-CoA (Fig. 3). Clearly, additional work on the phenylacetate pathway and on its integration with the hydroxyphenylacetate degradation pathways that are also operative is needed to define the full range of Paal biochemical function. Here we have merely demonstrated that the ring-hydroxylated phenylacetyl-CoA is the preferred substrate.

**Quaternary and Tertiary Structure of the Apo *E. coli* Paal**—The structure of apo *E. coli* Paal was determined to 2.0 Å of resolution (statistics are provided in Table 3, and electron density obtained from a simulated annealing omit map of the active site is represented in Fig. 4A) using crystals grown from the Seleno-Met protein at pH 6.0 in 13% polyethylene glycol, ammonium sulfate solution. The overall structure of the *E. coli* Paal protomer resembles that of several other proteins in the PDB as revealed by a search with the program DALI (66). *E. coli* Paal has the most structural and sequence similarity to PDB 1j1y, with a 1.3-Å root mean square deviation on 112 C $\alpha$  atoms with 36% sequence identity (Paal protein from *T. thermophilus* (49)). *E. coli* Paal is also similar to several other hot dog-fold thioesterases, although none exhibited sequence identities of greater than 24%. Among these is the *Arthrobacter* sp. strain SU 4-HBA-CoA thioesterase that will be the focus of the structure-function comparisons described below.

*E. coli* Paal, which is a tetramer in solution, crystallized with a dimer in the crystallographic asymmetric unit. Although the protomer structures appear similar, both the N- and C-terminal regions adopt different structures. In protomer A, the N-terminal  $\alpha$ -helix (amino acids 1–23) is continuous (Fig. 4B), whereas in protomer B the N-terminal  $\alpha$ -helix is

kinked at amino acid 16 (Fig. 4C). In addition, six additional amino acids are ordered in the electron density for protomer B.

The protomer topology is dominated by a 6-stranded anti-parallel  $\beta$ -sheet formed by amino acid residues 25–30, 33–39, 76–84, 93–103, 107–115, and 121–130 (Fig. 4, B and C). Residues 2–22 of the N terminus form an  $\alpha$ -helix (helix 1 in Fig. 4, B and C) that runs anti-parallel to  $\beta$ -strand A. The  $\beta$ -sheet wraps over one face of the second central  $\alpha$ -helix (helix 2 in Fig. 4, B and C); hence, the name “hot dog-fold.” Two protomers associate to form a continuous 12-stranded anti-parallel  $\beta$ -sheet, and this dimer associates back-to-back with a second dimer (Fig. 4D). The protomer-protomer interface is formed through interactions between respective  $\beta$ -strands (F) which orient anti-parallel (contacts exist between residues 78 and 84 and 80 and 82) and through interactions between the first two turns of the respective  $\alpha$ -helices (2), also oriented anti-parallel (contact is between residues 18 and 52).

The locations of the active sites in the *E. coli* Paal dimer are identified in Fig. 5A by the superposition of the structure of *T. thermophilus* Paal bound with hexanoyl-CoA at one active site (49) and in Fig. 5B by the superposition of the structure of *Arthrobacter* sp. strain SU 4-HBA-CoA thioesterase complexed with the inhibitor 4-hydroxyphenylacetyl-CoA at both active sites (40). The acyl-CoA ligand is bound at the protomer-protomer interface with the acyl-thioester moieties inserted into the core of the dimer. The ligand CoA units rest on the dimer surface. The 4-hydroxyphenylacetyl-CoA ligand (Structure 1) was shown to be a competitive inhibitor of the *A. Evansii* Paal with a  $K_i = 39 \mu\text{M}$  (Table 1).

**Catalytic Site of the *E. coli* Paal**—The residues forming the catalytic site of *E. coli* Paal are shown in Fig. 5C. The N-terminal  $\alpha$ -helix, which is linear in protomer A (Fig. 4B) and kinked in protomer B (Fig. 4C), forms one side of the active site. The helix conformation, thus, impacts on the constitution of the active site. In protomer A, the Glu-14 and Asn-15 side chains project into the catalytic site, whereas in protomer B they are directed to solvent. In contrast, in protomer B the Asp-16 is directed at the active site, whereas in protomer A it is solvated. Which protomer A or B is the best representative of the catalytically active conformation of the enzyme? To address this question, the three residues Glu-14, Asn-15, and Asp-16 were separately replaced with Ala by site-directed mutagenesis. The kinetic properties of the mutants were tested with the three substrates 3,4-dihydroxyphenylacetyl-CoA, 3-hydroxyphenylac-

**TABLE 3**  
Crystallographic data and refinement statistics

Cell constants	$a = b = 69.9 \text{ \AA}, c = 117.2 \text{ \AA}$
Space group	$P3_121$ , 2 molecules per asymmetric unit
X-ray source	APS 311D Beamline
PDB code	2FS2
<b>Se-Met peak data</b>	
Wavelength (Å)	0.9798
Resolution (Å)	20.0–2.0
Number of observations	99,872
Number of reflections <sup>a</sup>	40,460
Completeness (%) (2.07–2.0 Å) <sup>a</sup>	93.5 (88.9)
Average redundancy (2.07–2.0 Å) <sup>a</sup>	2.5 (2.2)
Mean $I/\sigma(I)$ (2.07–2.0 Å)	6.9 (1.4)
$R_{\text{merge}}$ on $I^b$ (2.07–2.0 Å)	9.3 (46.2)
Cut-off criteria	$I > -0.5 \sigma(I)$
SOLVE figure of merit <sup>c</sup>	0.21 (20.0–2.0 Å of resolution) for 19,074 reflections
RESOLVE Figure of merit <sup>c</sup> with 2-fold NCS	0.48 (20.0–2.6 Å of resolution) for 29,562 reflections
<b>Model and refinement statistics</b>	
Resolution range	20.0–2.0 Å
Number of reflections	19,072 (18,102 in working set; 970 in test set)
Completeness	83.1% (5.1% in test set)
Cutoff criterion	$F > 0.0$
Protein atoms	2016
Water atoms	79
Sulfate atoms	15
$R_{\text{cryst}}^d$ (2.05–2.0 Å)	0.187 (0.319)
$R_{\text{free}}^d$ (2.05–2.0 Å)	0.230 (0.366)
<b>Root mean square deviations</b>	
Bond lengths (Å)	0.031
Bond angles (Å)	2.3
Mean $B$ value/ $B$ factor root mean square deviation main chain/side chain (Å <sup>2</sup> )	32.9/1.7/4.8
<b>Ramachandran plot statistics<sup>e</sup></b>	
Residues in most favored regions	224 (93.3%)
Residues in additional allowed regions	16 (6.7%)
Residues in generously allowed regions	0 (0%)
Residues in disallowed regions	0 (0%)

<sup>a</sup> Data completeness treats Bijvoët mates independently.

<sup>b</sup>  $R_{\text{merge}} = \sum_{hkl} \sum_i |I(hkl)_i - \langle I(hkl) \rangle| / \sum_{hkl} \sum_i I(hkl)_i$ .

<sup>c</sup> Figure of merit was calculated using SOLVE/RESOLVE.

<sup>d</sup>  $R_{\text{cryst}} = \sum_{hkl} |F_o(hkl) - F_c(hkl)| / \sum_{hkl} |F_o(hkl)|$ , where  $F_o$  and  $F_c$  are observed and calculated structure factors, respectively.

<sup>e</sup> Calculated with PROCHECK.

etyl-CoA, and 4-hydroxyphenylacetyl-CoA (Table 2). Whereas the D16A mutant showed significantly reduced activity, the E14A and N15A mutants did not. Thus, protomer B appears to be the active conformer.

There are several ionizable residues located in the catalytic site of protomer B that might contribute to the pH rate profiles shown in Fig. 2. These include Asp-61, His-48, His-52, and Asp-16. Each of these residues is conserved in the *A. Evansii* and *T. thermophilus* Paals.

To gain insight into the possible functions of the active site residues in the *E. coli* Paal, the catalytic site of protomer B was superpositioned with the catalytic site of the *Arthrobacter* sp. strain SU 4-HBA-CoA thioesterase complexed with the inhibitor 4-hydroxyphenacyl-CoA (40) (Fig. 5D). The *E. coli* Paal residues that surround the reaction center are Asn-46, His-52, Gly-53, Asp-61, and Thr-62. It is known from earlier studies that two key catalytic residues in the 4-HBA-CoA thioesterase are Glu-73, which functions as a nucleophile or as a general base, and Gly-65, which engages in hydrogen-bond formation with the thioester C=O (40, 50, 67). The corresponding residues in the *E. coli* Paal are Asp-61 and Gly-53. To test the importance of Asp-61 to catalysis, it was replaced with Ala. A small but detectable level of catalytic activity was observed (Table 2) that was suspected to derive from the contamination of the mutant protein with the native *E. coli* Paal. To avoid potential

contamination issues, the *A. Evansii* Paal was utilized because it could be separated from the native *E. coli* Paal by fast protein liquid chromatography gel filtration chromatography (see “Materials and Methods”). Accordingly, the *A. Evansii* Paal D75A mutant was found to have no detectable activity. Thus, Asp-61, and by analogy Asp-75, are essential to *E. coli* and *A. Evansii* Paal catalysis, respectively. The *A. Evansii* Paal D75N mutant retained a small amount of activity (Table 1), which might be a reflection of the rate of attack by an oriented water molecule at the polarized thioester C=O.

The *E. coli* Paal His52 corresponds to the *Arthrobacter* 4-HBA-CoA thioesterase active site His-64 (Fig. 5D), which is positioned for hydrogen-bond interaction with the catalytic Glu-73. The His-52 is seen in two different rotomer conformations in the *E. coli* Paal (Fig. 5C), indicating some degree of conformational freedom in the unliganded active site. In unpublished work (68), catalysis by the *Arthrobacter* 4-HBA-CoA thioesterase H64A mutant was shown to be  $\sim 10^4$  less efficient than that of the wild-type enzyme ( $k_{\text{cat}}/K_m = 5 \times 10^6 \text{ M}^{-1}\text{s}^{-1}$  versus  $k_{\text{cat}}/K_m = 3 \times 10^2 \text{ M}^{-1}\text{s}^{-1}$ ). In the present study, *E. coli* Paal H52A-catalyzed hydrolysis of the hydroxylated phenylacetyl-CoAs was evaluated (Table 2). A  $10^3$ -fold decrease in the  $k_{\text{cat}}/K_m$  was observed with the 4-hydroxyphenylacetyl-CoA, and a  $10^2$ -fold decrease in the  $k_{\text{cat}}/K_m$  value was observed with the 3-hydroxyphenylacetyl-CoA or 3,4-dihydroxyphenylacetyl-CoA.

The *E. coli* Paal Asn-46 is positioned opposite to the Asp-61 (Fig. 5D), just as the Gln-58–Glu-73 pair is positioned in the *Arthrobacter* 4-HBA-CoA thioesterase (40) (Fig. 5D). To determine the contribution of the active site Asn-46 to Paal catalysis, it was replaced with Ala by site-directed mutagenesis. In addition, the corresponding residue Asn-60 in the *A. Evansii* Paal was replaced with Ala and with Asp. The kinetic properties of the mutants (Tables 1 and 2) indicate that the Asn side chain contributes significantly to the efficiency of catalytic turnover.

**Structural Basis for Paal Substrate Specificity**—Although 4-hydroxybenzoyl-CoA binds to the *A. Evansii* Paal active site (competitive inhibition constant  $K_i = 260 \mu\text{M}$ ; Table 1), it is not hydrolyzed. The Paal utilizes an Asp for general base (or nucleophilic) catalysis, whereas the 4-HBA-CoA thioesterase uses a Glu. Likewise, the Paal employs an Asn opposite to the catalytic carboxylate, whereas the 4-HBA-CoA thioesterase uses Gln (Fig. 5D). We asked the question, Does the Asn/Asp versus Gln/Glu control whether 3,4-dihydroxyphenylacetyl-CoA or 4-hydroxybenzoyl-CoA is the substrate? To address this question, the catalytic activity of the *E. coli* Paal N46Q/D61E double mutant was evaluated with these two thioesters serving as substrates. No activity was observed. We conclude from this result that the substrate specificity cannot be simply switched by swapping the paired active site residues. Indeed, the catalytic sites of the two enzymes differ in other aspects. Most notably, the active site Thr residues (Thr-62 in Paal and Thr-77 4-HBA-CoA thioesterase) are stationed differently; His-48 in Paal replaces Trp-60 in the 4-HBA-CoA thioesterase, and the residue flanking the catalytic carboxylate in the *E. coli* Paal is Ala-77 and Gly-93 in the 4-HBA-CoA thioesterase (Fig. 5D). Thus, substrate specificity derives from the composite of the active site residues. This is consistent with the observation that whereas the 4-hydroxyphenacyl-CoA ( $K_i = 39 \mu\text{M}$ ;  $K_i = 29 \mu\text{M}$  for the 3-hydroxyphenacyl-CoA) and 4-hydroxybenzoyl-CoA ( $K_i = 3.4 \text{ mM}$ ) analogs bind to Paal (Table 1), they do so with much reduced affinity than is observed for binding to the *Arthrobacter* 4-HBA-CoA thioesterase ( $K_i = 0.003 \mu\text{M}$  and  $K_i = 0.6 \mu\text{M}$ , respectively).

The preference that Paal shows for the 3- and 4-hydroxyphenylacetyl-CoA versus phenylacetyl-CoA (Tables 1 and 2) is striking. Inspection of the surface picture of the *E. coli* Paal (Fig. 6) with the 4-hydroxy-

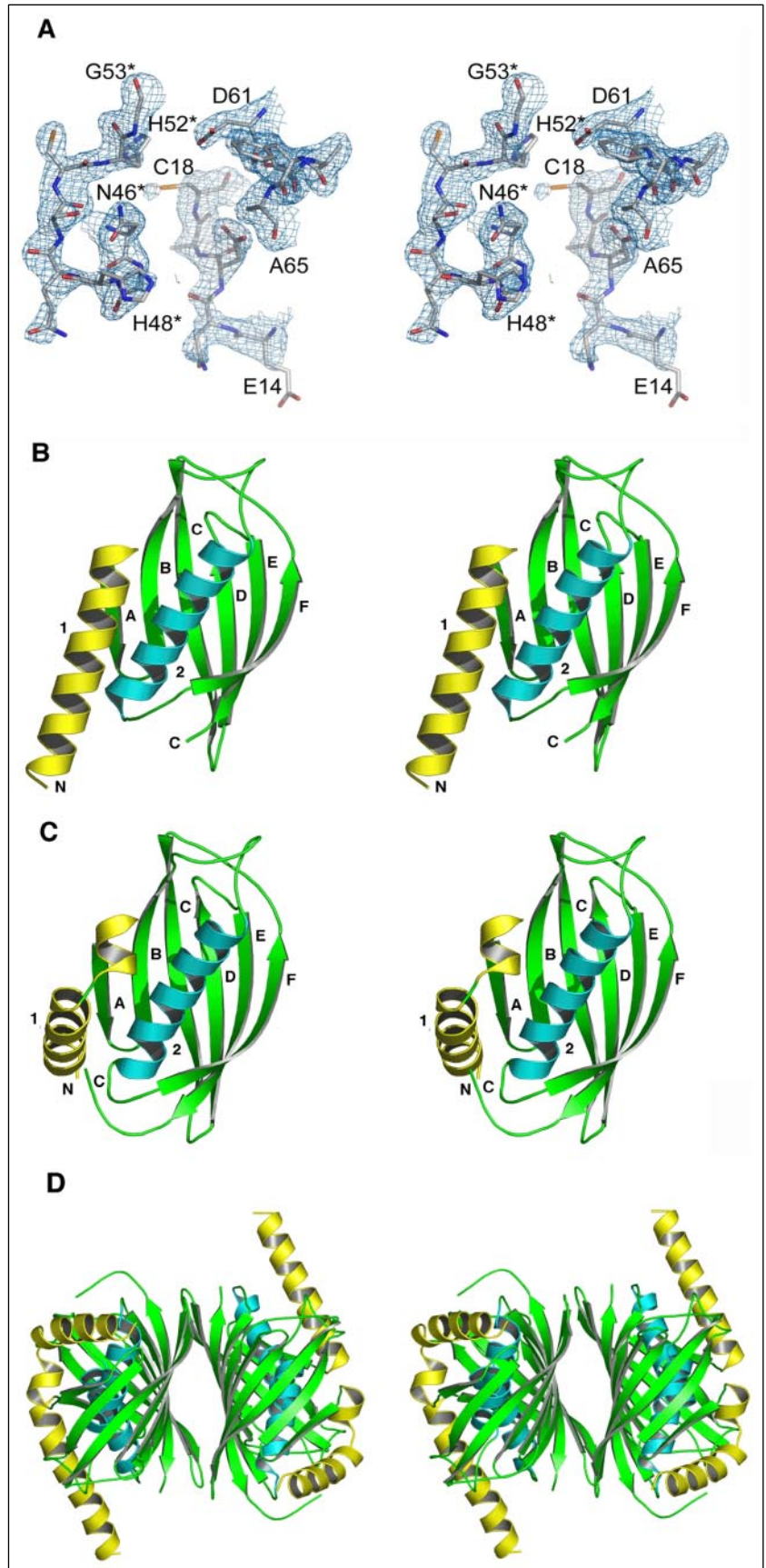


FIGURE 4. *A*, simulated annealing "omit" map is shown contoured around respective active site residues  $1.0\sigma$ . Calculated using CNS (60) by omitting 5% of the model for each round of refinement. Residues are labeled and numbered with *asterisks* indicating side chain positions emanating from the adjacent protomer in the dimer interface. Structural representations were prepared with PyMol unless otherwise indicated (69). *B* and *C*, the stereo pictures of *E. coli* Paal monomers, generated the coordinates deposited under PDB ID 1PSU and the graphics program Pymol (69). The  $\alpha$ -helices 1 and 2 are colored *yellow* and *cyan*. The  $\beta$ -strands A to F and the loops are colored *green*. The N and C termini are labeled. *D*, the stereo pictures of *E. coli* Paal tetramer, generated with the coordinates deposited under PDB code 1PSU and the graphics program Pymol (69). The  $\alpha$ -helices 1 and 2 are colored *yellow* and *cyan*. The  $\beta$ -strands A to F and the loops are colored *green*.

## Phenylacetate Pathway Thioesterase

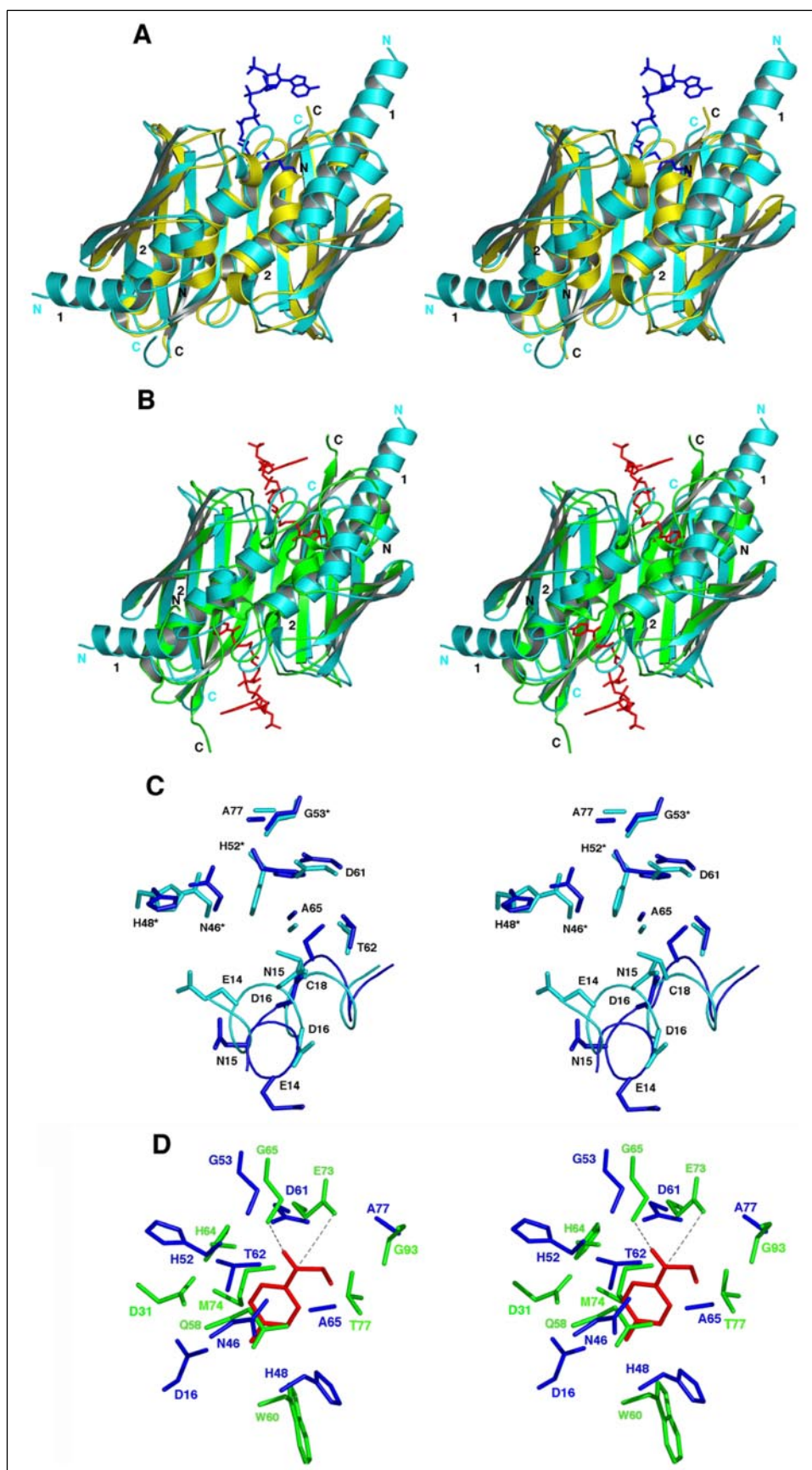


FIGURE 5. *A*, the stereo picture of the *E. coli* Paal (cyan) dimer overlaid with the *T. thermophilus* Paal dimer (yellow) bound with the ligand hexanoyl-CoA the type 2 orientation (blue) (49). The *E. coli* Paal N and C termini are cyan, and the *E. coli* Paal  $\alpha$ -helices 1 and 2 and the *T. thermophilus* Paal N and C termini are black. The figure was generated from the *E. coli* Paal (PDB code 1PSU) and *T. thermophilus* Paal (PDB ID 1WN3) using the graphics program Pymol (69). *B*, the stereo picture of the *E. coli* Paal (cyan) dimer overlaid with the *Arthrobacter* 4-HBA-CoA thioesterase dimer (green) bound with the ligand 4-hydroxyphenacyl-CoA. The *E. coli* Paal N and C termini are cyan, and the *E. coli* Paal  $\alpha$ -helices 1 and 2 and the *Arthrobacter* 4-HBA-CoA thioesterase N and C termini are as shown as black. The figure was generated from the *E. coli* Paal (PDB code 1PSU) and *Arthrobacter* 4-HBA-CoA thioesterase (PDB code 1Q4T) using the graphics program Pymol (69). *C*, stereo picture of the active site regions of *E. coli* Paal protomer A (cyan) and protomer B (blue). The residues E14, N15, D16, C18, D61, T62, A65, and A77 are from one subunit, whereas residues N46\*, H48\*, H52\*, and G53\* are from an adjacent subunit. The residues E14, N15, D16, and C18 are located on (N-terminal)  $\alpha$ -helix 1, and D61, T62, and A65 are located on (central)  $\alpha$ -helix 2. The residues N46, H48, and H52 are located on the connecting loop between  $\beta$ -strand B and  $\alpha$ -helix 2, and G53 is located at the N-terminal of  $\alpha$ -helix 2 (see Fig. 4, *B* and *C*). *D*, a stereo picture of *E. coli* Paal active site residues (blue) (protomer B) overlaid with *Arthrobacter* 4-HBA-CoA thioesterase active site residues (green) with truncated ligand 4-hydroxyphenacyl-CoA (red). The H-bond and the trajectories between the *Arthrobacter* 4-HBA-CoA thioesterase Glu-73 carboxylate oxygen and ligand benzoyl carbonyl carbon are indicated with black dashed lines. The *E. coli* Paal residues N46, H48, H52, G53, D61, T62, A65, and A77 correspond in their locations to the *Arthrobacter* 4-HBA-CoA thioesterase residues Q58, W60, H64, G65, E73, M74, T77, and G93, respectively.

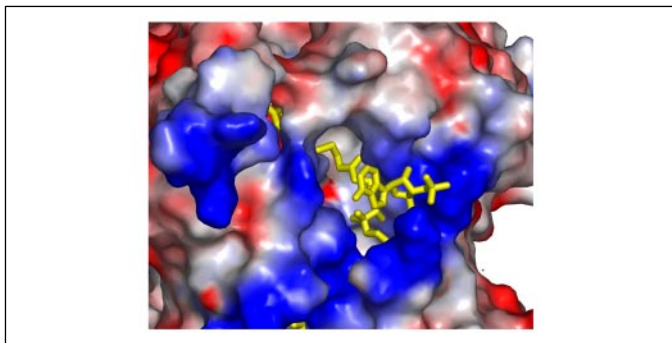


FIGURE 6. **Electrostatic surface picture illustrating the solvent exposure of *E. coli* Paal active site.** The active site is identified by the 4-hydroxyphenacyl-CoA ligand (yellow), which was positioned by superpositioning the Paal structure with the structure of the *Arthrobacter* 4-HBA-CoA thioesterase (4-hydroxyphenacyl-CoA) complex (PDB code 1Q4T) (40). The picture was generated using the graphics program Pymol (69).

phenacyl-CoA ligand (placed by the superimposition of liganded *Arthrobacter* 4-HBA-CoA thioesterase structure depicted in Figs. 5, B and D (40)) provides insight into why this might be the case. The aromatic ring of the ligand sits in a binding pocket that opens to solvent. The ring hydroxyl substituents might engage in interaction with nearby water molecules.

**Conclusions**—Paal shares the same branch of the evolutionary tree of the hot dog-fold thioesterase superfamily with the 4-HBA-CoA thioesterase from *Arthrobacter*. Paal has diverged to recognize the phenylacetyl-CoA core structure rather than the benzoyl-CoA core structure. Paal is most active with hydroxyphenylacetyl-CoA substrates. The partial exposure of the aromatic ring to solvent might account for this preference. Thus, by design or by accident, Paal can liberate CoA from phenylacetyl-CoA and from hydroxyphenylacetyl-CoA substrates that form from the phenylacetate pathway.

**Acknowledgments**—Use of the Advanced Photon Source is supported by the United States Department of Energy, Office of Science, Office of Basic Energy Sciences under Contract W-31-109-Eng-38. Use of the SGX Collaborative Access Team (SGX-CAT) beamline facilities at Sector 31 of the Advanced Photon Source was provided by Structural GenomiX, Inc., who constructed and operates the facility.

## REFERENCES

- Ramos, J. L., Gonzalez-Perez, M. M., Caballero, A., and van Dillewijn, P. (2005) *Curr. Opin. Biotechnol.* **16**, 275–281
- Diaz, E. (2004) *Int. Microbiol.* **7**, 173–180
- Parales, R. E., and Haddock, J. D. (2004) *Curr. Opin. Biotechnol.* **15**, 374–379
- Komives, T., and Gullner, G. (2005) *Z. Naturforsch.* **60**, 179–185
- D'Annibale, A., Ricci, M., Leonardi, V., Quarantino, D., Mincione, E., and Petruccioli, M. (2005) *Biotechnol. Bioeng.* **90**, 723–731
- Zhang, C., and Bennett, G. N. (2005) *Appl. Microbiol. Biotechnol.* **67**, 600–618
- Gibson, J., and Harwood, C. S. (2002) *Annu. Rev. Microbiol.* **56**, 345–369
- Samanta, S. K., Singh, O. V., and Jain, R. K. (2002) *Trends Biotechnol.* **20**, 243–248
- Peres, C. M., and Agathos, S. N. (2000) *Biotechnol. Annu. Rev.* **6**, 197–220
- Chaudhry, G. R., and Chapalamadugu, S. (1991) *Microbiol. Rev.* **55**, 59–79
- Hagblom, M. M. (1992) *FEMS Microbiol. Rev.* **9**, 29–71
- Poppe, L., and Retey, J. (2005) *Angew. Chem. Int. Ed. Engl.* **44**, 3668–3688
- Boyd, D. R., Sharma, N. D., O'Dowd, C. R., Carroll, J. G., Loke, P. L., and Allen, C. C. (2005) *Chem. Commun.* **31**, 3989–3991
- Boyd, D. R., Sharma, N. D., Llamas, N. M., Malone, J. F., O'Dowd, C. R., and Allen, C. C. (2005) *Org. Biomol. Chem.* **3**, 1953–1963
- Boyd, D. R., Sharma, N. D., Byrne, B. E., Haughey, S. A., Kennedy, M. A., and Allen, C. C. (2004) *Org. Biomol. Chem.* **2**, 2530–2537
- Diaz, E., Ferrandez, A., Prieto, M. A., and Garcia, J. L. (2001) *Microbiol. Mol. Biol. Rev.* **65**, 523–569
- Jimenez, J. L., Minambres, B., Garcia, L., and Diaz, E. (2002) *Environ. Microbiol.* **4**, 824–841
- Johnson, G. R., and Spain, J. C. (2003) *Appl. Microbiol. Biotechnol.* **62**, 110–123
- Bartolome-Martin, D., Martinez-Garcia, E., Mascaraque, V., Rubio, J., Perera, J., and Alonso, S. (2004) *Gene (Amst.)* **341**, 167–179
- Olivera, E. R., Minambres, B., Garcia, B., Muniz, C., Moreno, M. A., Ferrandez, A., Diaz, E., Garcia, J. L., and Luengo, J. M. (1998) *Proc. Natl. Acad. Sci. U. S. A.* **95**, 6419–6424
- Olivera, E. R., Reglero, A., Martinez-Blanco, H., Fernandez-Medarde, A., Moreno, M. A., and Luengo, J. M. (1994) *Eur. J. Biochem.* **221**, 375–381
- Luengo, J. M., Garcia, J. L., and Olivera, E. R. (2001) *Mol. Microbiol.* **39**, 1434–1442
- Ferrandez, A., Minambres, B., Garcia, B., Olivera, E. R., Luengo, J. M., Garcia, J. L., and Diaz, E. (1998) *J. Biol. Chem.* **273**, 25974–25986
- Mohamed, M. E.-S., Ismail, W., Heider, J., and Fuchs, G. (2002) *Arch. Microbiol.* **178**, 180–192
- Rost, R., Haas, S., Hammer, E., Herrmann, H., and Burchhardt, G. (2002) *Mol. Genet. Genomics* **267**, 656–663
- Gescher, J., Zaar, A., Mohamed, M., Schagger, H., and Fuchs, G. (2002) *J. Bacteriol.* **184**, 6301–6315
- Alonso, S., Bartolome-Martin, D., del Alamo, M., Diaz, E., Garcia, J. L., and Perera, J. (2003) *Gene (Amst.)* **319**, 71–83
- Martinez-Blanco, H., Reglero, A., Rodriguez-Aparicio, L. B., and Luengo, J. M. (1990) *J. Biol. Chem.* **265**, 7084–7090
- Mohamed, M. E.-S. (2000) *J. Bacteriol.* **182**, 286–294
- Ferrandez, A., Garcia, J. L., and Diaz, E. (2000) *J. Biol. Chem.* **275**, 12214–12225
- Garcia, B., Olivera, E. R., Minambres, B., Carnicero, D., Muniz, C., Naharro, G., and Luengo, J. M. (2000) *Appl. Environ. Microbiol.* **66**, 4575–4578
- Ismail, W., Mohamed, M. E.-S., Wanner, B. L., Datsenko, K. A., Eisenreich, W., Rohdich, F., Bacher, A., and Fuchs, G. (2003) *Eur. J. Biochem.* **270**, 3047–3054
- Gescher, J., Eisenreich, W., Worth, J., Bacher, A., and Fuchs, G. (2005) *Mol. Microbiol.* **56**, 1586–1600
- Zaar, A., Gescher, J., Eisenreich, W., Bacher, A., and Fuchs, G. (2004) *Mol. Microbiol.* **54**, 223–238
- Holden, H. M., Benning, M. M., Haller, T., and Gerlt, J. A. (2001) *Acc. Chem. Res.* **34**, 145–157
- Haller, T., Buckel, T., Retey, J., and Gerlt, J. A. (2000) *Biochemistry* **39**, 4622–4629
- Leesong, M., Henderson, B. S., Gillig, J. R., Schwab, J. M., and Smith, J. L. (1996) *Structure* **4**, 253–264
- Dillon, S. C., and Bateman, A. (2004) *BMC Bioinformatics* **5**, 109–122
- Zhuang, Z., Gartemann, K.-H., Eichenlaub, R., and Dunaway-Mariano, D. (2003) *Appl. Environ. Microbiol.* **69**, 2707–2711
- Thoden, J. B., Zhuang, Z., Dunaway-Mariano, D., and Holden, H. M. (2003) *J. Biol. Chem.* **278**, 43709–43716
- Scholten, J. D., Chang, K.-H., Babbitt, P. C., Charest, H., Sylvestre, M., and Dunaway-Mariano, D. (1991) *Science* **253**, 182–185
- Zhuang, Z., Song, F., Takami, H., and Dunaway-Mariano, D. (2004) *J. Bacteriol.* **186**, 393–399
- Hunt, M. C., and Alexson, S. E. (2002) *Prog. Lipid Res.* **41**, 99–130
- Yu, W., Liang, X., Ensenauer, R. E., Vockley, J., Sweetman, L., and Schulz, H. (2004) *J. Biol. Chem.* **279**, 52160–52167
- Ren, Y., Aguirre, J., Ntamack, A. G., Chu, C., and Schulz, H. (2004) *J. Biol. Chem.* **279**, 11042–11050
- Duncan, J. A., and Gilman, A. G. (1998) *J. Biol. Chem.* **273**, 15830–15837
- Mumby, S. M., Kleuss, C., and Gilman, A. G. (1994) *Proc. Natl. Acad. Sci. U. S. A.* **91**, 2800–2804
- Hunt, M. C., Solaas, K., Kase, B. F., and Alexson, S. E. (2002) *J. Biol. Chem.* **277**, 1128–1138
- Kunishima, N., Asada, Y., Sugahara, M., Ishijima, J., Nodake, Y., Sugahara, M., Miyano, M., Kuramitsu, S., Yokoyama, S., and Sugahara, M. (2005) *J. Mol. Biol.* **352**, 212–228
- Thoden, J. B., Holden, H. M., Zhuang, Z., and Dunaway-Mariano, D. (2002) *J. Biol. Chem.* **277**, 27468–27476
- Luo, L., Taylor, K. L., Xiang, H., Wei, Y., Zhang, W., and Dunaway-Mariano, D. (2001) *Biochemistry* **40**, 15684–15692
- Merkel, S. M., Eberhard, A. E., Gibson, J., and Harwood, C. S. (1989) *J. Bacteriol.* **171**, 1–7
- Theilacker, W., and Schmid, W. (1950) *Annalen* **570**, 15–33
- Hendrickson, W. A., Horton, J. R., and LeMaster, D. M. (1990) *EMBO J.* **9**, 1665–1672
- Otwinowski, Z., and Minor, W. (1997) *Methods Enzymol.* **276**, 307–326
- Collaborative Computational Project, Number 4 (1994) *Acta Crystallogr. D Biol. Crystallogr.* **50**, 760–763
- Terwilliger, T. C., and Berendzen, J. (1999) *Acta Crystallogr. D Biol. Crystallogr.* **55**, 849–861
- Terwilliger, T. C. (2000) *Acta Crystallogr. D Biol. Crystallogr.* **56**, 965–972
- Jones, T. A., Zou, J. Y., Cowan, S. W., and Kjeldgaard, M. (1991) *Acta Crystallogr. A* **47**, 110–118
- Brunger, A. T., Adams, P. D., Clore, G. M., DeLano, W. L., Gros, P., Grosse-Kunstleve, R. W., Jiang, J. S., Kuszewski, J., Nilges, M., Pannu, N. S., Read, R. J., Rice, L. M.,

## Phenylacetate Pathway Thioesterase

- Simonson, T., and Warren, G. L. (1998) *Acta Crystallogr. D Biol. Crystallogr.* **54**, 905–921
61. Erlich, H. A. (1991) *PCR Technology: Principles and Applications for DNA Amplification*, W. H. Freeman and Co., New York, NY
62. Bradford, M. M. (1976) *Anal. Biochem.* **72**, 248–254
63. Fersht, A. (1990) *Structure and Mechanism in Protein Science*, pp. 164–168, W. H. Freeman and Co., New York, NY
64. Zaar, A., Eisenreich, W., Bacher, A., and Fuchs, G. (2001) *J. Biol. Chem.* **276**, 24997–25004
65. Alonso, M. J., Bermejo, F., Reglero, A., Fernandez-Canon, J. M., Gonzalez de Buitrago, G., and Luengo, J. M. (1988) *J. Antibiot. (Tokyo)* **41**, 1074–1084
66. Holm, L., and Sander, C. (1993) *J. Mol. Biol.* **233**, 123–138
67. Zhuang, Z., Song, F., Zhang, W., Taylor, K., Archambault, A., Dunaway-Mariano, D., Dong, J., and Carey, P. R. (2002) *Biochemistry* **41**, 11152–11160
68. Zhuang, Z. (2003) *Structure-Function Relationship within the 4-Hydroxybenzoyl-CoA Thioesterase Enzyme Superfamily*. Ph.D. dissertation, University of New Mexico, Albuquerque, NM
69. DeLano, W. L. (2002) *The PyMOL User's Manual*, DeLano Scientific, San Carlos, CA